

Understanding domain-wall encoding theoretically and experimentally

Jesse Berwald,¹ Nicholas Chancellor,^{1, 2, *} and Raouf Dridi¹

¹*Quantum Computing Inc. Leesburg, VA, USA*

²*Physics department, Durham University Physics department Quantum Light and Matter section and Durham-Newcastle Joint Quantum Centre, South Road, Durham UK*

We analyze the performance of encoding pairwise interactions of higher-than-binary discrete variables (these models are sometimes referred to as discrete quadratic models) into binary variables based on domain walls on one dimensional Ising chains. We discuss how this is relevant to quantum annealing, but also many gate model algorithms such as VQE and QAOA. We theoretically show that for problems of practical interest for quantum computing and assuming only quadratic interactions are available between the binary variables, it is not possible to have a more efficient general encoding in terms of number of binary variables per discrete variable. We furthermore use a D-Wave Advantage 1.1 flux qubit quantum annealing computer to show that the dynamics effectively freeze later for a domain-wall encoding compared to a traditional one-hot encoding. This second result could help explain the dramatic performance improvement of domain wall over one hot which has been seen in a recent experiment on D-Wave hardware. This is an important result because usually problem encoding and the underlying physics are considered separately, our work suggests that considering them together may be a more useful paradigm. We argue that this experimental result is also likely to carry over to a number of other settings, we discuss how this has implications for gate-model and quantum-inspired algorithms.

I. INTRODUCTION

Quantum computing shows great promise for combinatorial optimisation problems, and many proof-of-concept experiments have been performed demonstrating the potential in a variety of areas including vehicle scheduling [1], traffic flow optimisation [2, 3], hydrology [4], computational biology [5, 6], community detection [7], graph theoretical problems [8–10], and supply chain logistics [11]. While this is an area with great promise, available devices exist in relatively early stages of development, which is often termed the noisy intermediate-scale quantum (NISQ) [12] era of quantum computing. In these early stages, it is crucial to be able to get the most out of these devices through, among other things, optimal encoding of problems.

Currently there are two major paradigms of quantum computing, analog quantum computing, typified by quantum annealing computers, and employing continuous time evolution, and digital gate model quantum computing which performs a series of discrete “gate” operations. In both settings, it is crucial to use the hardware optimally, including optimal encoding of problems, but the constraints may be different. In particular, the physical interactions underlying the operation of these devices typically do not involve more than two qubits, so it is natural to consider optimisation problems which can be expressed as a quadratic problem, those which only involve single binary variable terms

and interactions between pairs of binary variables. One example of particular interest here are quadratic unconstrained binary optimisation problems (QUBOs). It is

always possible to map an optimisation problem involving higher order interactions into a QUBO, but this will come at a cost in terms of “auxilliary” variables which must be added to engineer the interactions [13–15]. In the case of gate model quantum computers, it is also possible to engineer these higher order interactions out of a sequence of pairwise interactions, without having to add more qubits. For example, a sequence of CNOT gates can map the total parity of an arbitrary number of qubits to a single qubit value.

In this work, we study the specific case where problems involve higher-than-binary discrete variables, which must be mapped to binary variables [51]. One way to approach this problem is binary encoding, where each value of the discrete variable is assigned a bitstring and the number of binaries used is the minimum allowed by information theory. Another approach is to use a unary encoding for each discrete variable, such that the number of binary variables used to encode grows linearly with the size of the discrete variable. The two common methods used here are one-hot and domain-wall encoding [16].

Both of these encodings and a few other specific examples will be discussed in detail in the next section. It is worth remarking that while a single variable encoding using unary methods is not a scalable way to build a quantum computer, a setting where the number of such variables is increased as the problem size is scaled up does meet the criteria for scalability as discussed in [17].

In this paper we consider these encodings at the level of problem mapping, meaning that we assume that the problem should be expressed directly as a QUBO. This is a realistic assumption in the setting of quantum annealing, but may not be for gate model quantum computing, where there may be other compilation methods available. As [18] illustrates, that leads to complicated trade-offs which will not be discussed here.

*Electronic address: nicholas.chancellor@gmail.com

The first key result we find is that in the quadratic setting, the domain-wall encoding is the most efficient possible encoding in terms of binary variable number for practical problems if arbitrary interactions between the discrete variables are desired. This result includes not only one-hot and binary encodings, but also any hypothetical, yet-to-be-discovered encodings which may use an intermediate number of binary variables per discrete variable.

The second major result of this paper is to gain a better understanding of why the domain-wall encoding experimentally out-performs one-hot in recent quantum annealing experiments [10]. By performing

experiments on a D-Wave Advantage 1.1 quantum annealing computer, we find that this is due to a combination of factors, including the fact that fewer binary variables induces a smaller solution space, and therefore reduces the effect of thermal fluctuations, as well as the fact that the annealing dynamics effectively “freeze” later in the anneal, meaning that the dynamics are more conducive to computation. The second of these effects was theoretically predicted in [16], due to the fact that only a single binary variable needs to be flipped to change the value of the discrete variable in the domain-wall encoding, while two need to be flipped in the one-hot setting. These results rely on a simplified version of a problem known as the quadratic assignment problem (QAP), and modeling based on the celebrated Kibble-Zurek mechanism [19, 20]. This mechanism has previously been studied as a model of programmable quantum annealing computers [21–23]. In particular, [21] used the same model of instantaneous freezing we use here, but for a problem where both the effects of quantum and thermal fluctuations were frozen in. We show that for the experiments here a model based only on thermal fluctuations at the freeze time is a valid approximation.

II. BACKGROUND

A. Flux qubit quantum annealing computer

The experiments reported here are performed on a D-Wave Advantage 1.1 programmable flux qubit quantum annealing computer. These devices produce a fully programmable transverse field Ising model on a restricted hardware graph χ . The effective Hamiltonian of the device takes the form

$$H(s) = -A(s) \sum_i X_i + B(s) \left(\sum_{i,j \in \chi} J_{ij} Z_i Z_j + \sum_i h_i Z_i \right) \quad (1)$$

where X and Z are Pauli matrices and $0 \leq s \leq 1$ is the annealing parameter which controls the anneal such that $A(s)$ monotonically decreases and $B(s)$ monotonically increases, as depicted in figure 1. Since we only consider forward annealing protocols without schedule

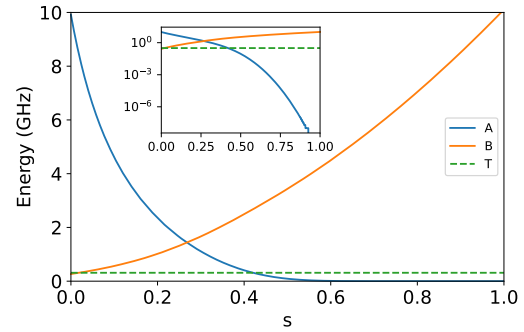


FIG. 1: Annealing schedule for the D-Wave Advantage 1.1 processor showing the A (decreasing with increasing s), and B (decreasing with increasing s) curves along with the temperature ($\approx 15 \text{ mK} \approx 0.31 \text{ GHz}$). The inset is the same plot but with a logarithmic scale on the y-axis.

variations in this paper, $s = \frac{t}{t_{\text{anneal}}}$ where t is time and $t_{\text{anneal}} = 20 \mu\text{s}$, which is the default value for these devices. It is worth noting that, while not conventionally included in the Hamiltonian, there is also significant thermal dissipation within the circuit. Since optimal solutions are mapped to low energy states, this dissipation can play a positive role, in fact it was even shown in [24] that energy increases due to thermal fluctuations can lead to improved performance. There are also negative effects from the interaction with the environment, including thermodynamic effects related to sampling a finite temperature distribution [25], the effects of finite temperature play an important role in the results reported here.

The optimisation problems which these devices solve are programmed into the B terms of equation 1. Equivalently, these problems can be considered as QUBO problems, by realizing that the bit value $b \in \{0, 1\}$ can be encoded as $b = \frac{1-Z}{2}$, where the allowed measurement values of Z are $\{1, -1\}$. Note that if we think of the measurement value of Z it can be treated as a classical binary variable $\sigma \in \{1, -1\}$, since we are most interested in the higher level picture of the problem not including detailed annealing dynamics we use σ for the remainder of the paper. Because the problems we are considering will usually not be subgraphs of the hardware graph χ , we map the problem using minor embedding [26, 27]. We use the “uniform torque compensation” [28] heuristic which is provided as part of the D-Wave Ocean software suite to determine the strength of the minor embedding chains.

B. Unweighted quadratic assignment problem

For the experimental results presented here, we study an unweighted version of the quadratic assignment problem. In other words we consider a version where all combinations of facilities and locations have an equal cost. This version of the QAP is no longer a hard combinatorial problem, but it is still a challenging optimization task due to the large number of variables and constraints.

rial optimisation problem, since all feasible assignments are equally optimal, and a feasible assignment can be found (for example) by assigning the first facility to a location at random and then iteratively performing assignments based on the lists of remaining facilities and locations.

While not a direct test of the ability of the annealing computer to solve hard combinatorial optimisation problems, this problem can act as an indirect test, since the ability to find feasible solutions (by which we mean solutions where one facility is assigned to one location and vice-versa) is an important step on the way to finding optimal solutions, such as in optimality certificate-based approaches, e.g., Graver basis [29]. Moreover, since the unweighted version of this problem is symmetric with respect to permutations of the facilities and locations, it is easier to perform thermal sampling using Monte Carlo methods. This follows from the fact that sampling the solution space around one feasible solution is the same as sampling around any other—the solution space is a single orbit under the permutations group action.

Moreover, the basic structure of the double constraint, one facility per location, and one location per facility is the same as the underlying constraint in a travelling salesperson (TSP) problem. Consider the placement of the order in which each city is visited in the journey (first, second, third, etc...). Then the constraint that each city can be visited only once is equivalent to saying that each city must have a unique placement in the order of the journey (the same city cannot be both first and third for example). The constraint that each city must be visited at least once can then be enforced by allowing each placement in the order to be used only once (for example only a single city can be third in the order).

For the TSP the distances between cities become additional quadratic interactions between the discrete variables. For the (weighted) QAP, the cost of each assignment appears as a linear term on discrete variables. This distinction is important because it means that the graph structure of the underlying QUBO (and therefore the minor embedding used when mapping to a quantum annealing computer) will be unchanged when weights are added to the QAP in the domain-wall or one-hot encoding (since these will be linear), but will be if the unweighted QAP is transformed into a TSP as described in the previous paragraph.

C. Discrete Quadratic Models (DQMs) and encoding to binary variables

Many important optimisation problems which exist in the real world involve discrete variables which are higher than binary. In other words, they involve variables which belong to m distinct classes, where $m > 2$. For the QAP, each facility can be placed at any location, so this can also be expressed by discrete variables. Problems which can be expressed as discrete variables with arbitrary pairwise

interactions are conventionally called discrete quadratic models, which we abbreviate as DQM.

To express the QAP (or TSP) as a DQM, either constraint can be used. For instance, we can either define the DQM variables as the choice of facilities for each location (the order in which each city appears for TSP) or equivalently as the choice of location for each facility (which city appears at each placement in the order for the TSP). In both cases, additional constraints must be added to the DQM to guarantee that the discrete variables take unique values.

Following the convention in [10], we define DQMs based on a collection of two index variables, $x_{i,\alpha}$, where the index i refers to the variable number, and the index α refers to the variable's class. An arbitrary DQM is then defined by the following Hamiltonian,

$$H_{\text{DQM}} = \sum_{i,j} \sum_{\alpha,\beta} D_{(i,j,\alpha,\beta)} x_{i,\alpha} x_{j,\beta} \quad (2)$$

where $D_{(i,j,\alpha,\beta)}$ are the pairwise interactions which determine the overall energy of a configuration.

An unweighted QAP can be defined by setting $D_{(i,j,\alpha,\alpha)} = 1 \ \forall \alpha, i > j$. However it is worth noting that this definition is not unique because $x_{i,\alpha} x_{i,\beta} = 0 \ \forall \alpha \neq \beta$, so any finite value of $D_{(i,i,\alpha,\beta)}$ with $\alpha \neq \beta$ does not change the underlying problem. A computationally interesting QAP will also include values of $D_{(i,i,\alpha,\alpha)}$ corresponding to the cost of each facility/location combination and will require $D_{(i,j,\alpha,\alpha)} = \kappa \ \forall \alpha, i > j$, where κ takes a large enough positive value to enforce the constraint. Similarly a TSP can be defined using the same constraint but taking $D_{(i,j,\alpha>\beta,\beta)}$ values corresponding to distances between cities. By this logic the unweighted QAP can also be thought of as an (unphysical) version of the TSP where the distance between all cities is zero.

a. One-hot constraints: Perhaps the simplest way to express a DQM as binary variables is to apply a constraint so that only a single variable can take the value 1 and enforce that all others take 0 values. This constraint can be realized as

$$H_{\text{one-hot}} = \kappa \left(\sum_{\alpha} b_{\alpha} - 1 \right)^2, \quad (3)$$

where $b_{\alpha} \in \{0, 1\}$ is a binary variable corresponding to each possible value, and $\kappa > 0$ is the constraint strength. In this method, if variables also are indexed by i there is a one-to-one correspondence between QUBO variables $b_{i,\alpha}$ and DQM variables $x_{i,\alpha}$. This correspondence makes it tempting to consider the one-hot encoding not as an encoding at all, but simply as constraints on binary variables (this is the way in which we introduced the QAP and TSP in section II B), each of which correspond to a specific value of a specific variable. However, this way of thinking about problems is no longer useful when no such one-to-one correspondence exists. This is the case for the other two encoding methods we discuss. Since

one-hot can also be thought of as an encoding of a DQM (although a rather trivial one), this way of thinking about it is more useful to compare it to other methods on the same footing.

b. k-hot constraints: A natural extension to the one-hot constraint is to consider the more general case where

$$H_{k\text{-hot}} = \kappa \left(\sum_{\alpha} b_{\alpha} - k \right)^2, \quad (4)$$

where k is an integer between 1 and $m - 1$. These constraints only allow states where k of the binary variables take the 1 value. Quadratic interactions must take the form $b_{i,\alpha} b_{j,\beta}$, and linear terms do not add independent degrees of freedom ($\sum_{\beta} b_{i,\alpha} b_{j,\beta} \propto b_{i,\alpha} + C$, where C is an irrelevant offset). For a k -hot encoding where each discrete variable is encoded into n_{var} binary variables there will be $\binom{n_{\text{var}}}{k}$ possible configurations while quadratic and linear interactions only add $n_{\text{var}}^2 + 2n_{\text{var}}$ independent degrees of freedom while $\binom{n_{\text{var}}}{k}^2 - 1$ degrees of freedom are available (assuming each quadratic term within a variable is independent). It follows that (except for possibly in small instances) quadratic and linear terms can only realize general interactions for $k = 1$ (one-hot) and $k = n_{\text{var}} - 1$ (one-hot with the definition of 0 and 1 reversed) where $\binom{n_{\text{var}}}{k} = k$. These constraints are still very useful because the form of interactions between the discrete variables encode a structure where each of the binary variables taking a value of 1 represents identical assets to be allocated, for example if k identical pieces of equipment must be allocated over a total of n_{var} locations.

c. Integral encodings: Integral encodings can be thought of as products of k -hot encodings. Taking the specific form

$$H_{\text{integral}} = \kappa \prod_{q=1}^R \left(\sum_{\alpha} b_{\alpha} - k_q \right)^2 \quad (5)$$

where the coefficients k should be integers in the range 0 to m , i.e. $k \in \mathcal{Z}_R$. The $R = 1$ case is a k -hot encoding, but for all $R > 1$ this constraint will require terms of order $2R$, which have to be realized by quadratization. Since k -hot encodings are not able to realize general interactions without higher than quadratic terms (assuming each state maps to a unique bitstring), integral encoding will not be able to either.

d. Domain-wall encoding: Another recently proposed method to encode DQMs is the domain-wall encoding [16]. In this encoding, for a discrete variable m , only $m - 1$ "spin" binary variables $\sigma_{\alpha} \in \{1, -1\}$ (the term "spin" derives from condensed matter physics where the direction of the magnetic spin of a spin $\frac{1}{2}$ particle is often denoted in this way). The values encode a domain-wall location (a point where the value of σ goes from -1 to 1) in a frustrated segment of a ferromagnetic spin chain.

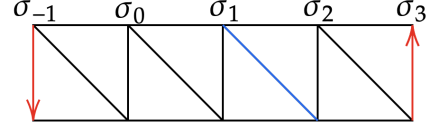


FIG. 2: Domain-wall encodings can be represented by triangulations of the Möbius strip. The number of squares represents the integer number m , and the blue twist gives the domain-wall location. Here $m = 4$ and the encoded value is $|\downarrow\downarrow\uparrow\rangle$.

In other words, the Hamiltonian is defined as

$$H_{\text{domain-wall}} = -\kappa \sum_{\alpha=-1}^{m-2} \sigma_{\alpha} \sigma_{\alpha+1}, \quad (6)$$

where the variables are defined for $\alpha \in \{0, m - 2\}$ and boundary conditions are enforced by setting $\sigma_{-1} = -1$ and $\sigma_{m-1} = 1$ (κ is again the constraint strength). An advantage of this encoding is that the DQM terms $x_{i,\alpha}$ can be expressed in a way which is linear in the σ variables:

$$x_{i,\alpha} = \frac{1}{2} (\sigma_{i,\alpha} - \sigma_{i,\alpha-1}). \quad (7)$$

Because $x_{i,\alpha}$ translates to a linear term in the domain wall encoding, it follows that $x_{i,\alpha} x_{j,\beta}$ will be quadratic in σ , therefore the domain-wall encoding of a DQM is always also quadratic in the underlying binary variables. Note that the notation here is identical to that used in [10] except for the fact that we use σ in place of s to avoid confusion with $s = \frac{t}{t_{\text{anneal}}}$. It is also worth remarking, that although not the subject of this paper, the domain-wall encoding has potential in simulating quantum field theories [30, 31].

A pictorial description of the domain-wall encoding is provided by triangulations of the Möbius Strip – See Figure 2.

e. Binary encoding: In terms of number of binary variables used to encode a discrete variable, the most efficient method to encode a DQM is to use binary encoding, in other words to assign each value of the discrete variable a bitstring. This method uses $\lceil \log_2(m) \rceil$ binary variables to encode variables of size m . To encode a DQM variable x_{α} , we must assign it a bitstring $r^{(\alpha)}$, where $r_q^{(\alpha)} \in \{0, 1\}$ is the value the bitstring takes on binary variable q . The encoding of a DQM therefore becomes

$$x_{i,\alpha} = \prod_{q=0}^{\lceil \log_2(m) \rceil - 1} \left(b_{i,\alpha} r_q^{(\alpha)} + (1 - b_{i,\alpha})(1 - r_q^{(\alpha)}) \right), \quad (8)$$

where again $b_{i,\alpha} \in \{0, 1\}$.

This encoding is not generally quadratic for $m > 2$ (it may happen that higher order terms cancel in special

cases though). Therefore, in order to translate a binary encoding of a DQM into a QUBO, we must also quadratize higher order terms. In other words, we must transform any terms of the form $b_{i,\alpha}b_{j,\beta}b_{k,\gamma}\dots$ to one which only has terms of the form $b_{i,\alpha}b_{j,\beta}$. There are multiple methods to translate higher order interactions into quadratic ones, but all require adding at least one auxilliary variable [13–15]. The optimal quadratization, i.e., quadratization with the minimum number of auxilliary variables, is NP-hard since the problem translates into computing a Groebner basis of a toric ideal [32]. A fair comparison between binary encoding and other methods such as one-hot and domain wall, has to include these extra variables. It was shown in [10] that, at least for one approach to quadratization, after these variables are taken into account, binary encoding of the specific colouring problems studied in that paper is less efficient than one-hot or domain-wall. In this paper we show a more general result based on degree-of-freedom counting, that for problems of more than three variables, there is no encoding strategy for which binary encoding uses fewer discrete variables than domain-wall encoding (which in turn uses fewer than one-hot).

f. Other encodings: While we are not aware of any other encoding methods to translate DQMs into QUBOs, it is possible that others could exist which use n_{var} binary variables where $\lceil \log_2(m) \rceil < n_{\text{var}} < m - 1$. In principle such encodings could always be constructed by taking a binary encoding and adding auxilliary variables which are constrained by the values the variables used in the binary encoding take. For this reason, we consider the possibility of using such encodings in our degree-of-freedom counting analysis as well. Since our analysis is performed from a perspective of counting degrees of freedom, the details of the encoding are not necessary to bound the number of binary variables required.

D. From one-hot to domain wall

Since a domain-wall encoding encodes the same information as a set of binary variables which are subject to a one-hot constraint, it is always possible to transform between the two. The recipe is as follows:

1. Identify all sets of one-hot constrained variables which need to be replaced and translate to a discrete quadratic model (DQM)
2. For each DQM variable, choose an order in which the values will be physically encoded on the chain used for the domain-wall encoding, this is necessary since, while one-hot constraints are permutation symmetric, the domain-wall encoding is not.
3. Generate the necessary domain-wall encodings for each DQM variable.
4. Translate DQM interactions into quadratic and binary terms acting on the new variables.

While it is most intuitive to think of the domain-wall encoding in terms of spin variables σ as discussed in section II C, optimisation problems are usually formulated as QUBOs. To allow easier comparison between the one-hot version (already formulated as a QUBO) and the domain-wall encoding we formulate this encoding as a QUBO as well, using the translation,

$$\sigma_{i,\alpha} = 1 - 2b_{i,\alpha}, \quad (9)$$

where $\sigma_{i,\alpha} \in \{1, -1\}$ is a spin variable and $b_i \in \{0, 1\}$ is a QUBO variable. In this new formulation, we define a DQM variable $x_{i,\alpha}$ as

$$x_{i,\alpha} = \frac{1}{2}(\sigma_{i,\alpha} - \sigma_{i,\alpha-1}) = b_{i,\alpha-1} - b_{i,\alpha}. \quad (10)$$

Furthermore the domain-wall constraint can be translated as,

$$H_{\text{chain}} = -\kappa \left(\sum_{\alpha=-1}^{m-2} 1 - 2b_{i,\alpha} - 2b_{i,\alpha+1} + 4b_{i,\alpha}b_{i,\alpha+1} \right), \quad (11)$$

where the pinned boundary values become $b_{i,\alpha=0} = 1$ and $b_{i,\alpha=m-1} = 0$.

The new QUBO generated by this translation has effectively turned half of the one-hot encoding into a domain-wall encoding. The remaining one-hot constraints end up acting like colouring constraints on a fully connected graph, effectively preventing any of the domain-walls from sitting on the same location in the chain and therefore preventing any of the encoded DQM variables from taking the same values.

One might be curious if it is possible to construct an encoding where both sets of one-hot constraints are translated into domain-wall constraints simultaneously, thereby reducing the number of binary variables to $(m - 1)^2$ rather than $m(m - 1)$. The degree-of-freedom-counting argument in section III A suggests that this is not likely to be possible.

III. RESULTS

A. Efficiency of domain-wall technique

While the experimental results reported in this paper all involve the domain-wall and one-hot encodings, it is worth reflecting on whether a direct binary encoding (or some other known encoding) could be more efficient in terms of number of binary variables used, or whether there are room for other, yet-to-be-discovered encodings which could beat the efficiency of the domain-wall encoding. We restrict ourselves to the question of encoding general interactions, in other words encodings which can assign arbitrary energies based on the value of the two variables. This is an important restriction, since binary encoding is known to be efficient for specific interactions,

for example in the case of the shortest vector problem [33].

We find however for general quadratic interactions that, for problems with four or more variables (as all interesting combinatorial optimisation problems will have), the domain-wall encoding is more efficient than any known encoding including binary, moreover, we rule out the possibility of any yet-to-be-discovered encoding which is more efficient. We do this using degree-of-freedom counting arguments similar to [16]. To start with we consider the case where auxilliary variables are not allowed, in other words, the interaction must be encoded directly in the linear and quadratic degrees of freedom of the binary variables used to encode discrete variables and do not allow additional binary variables to be added. We later generalize to the case where auxilliary variables are allowed and find the same conclusion, that the domain wall encoding is the most efficient. For simplicity we assume that all discrete variables are of size m , although in principle the arguments here could be extended to problems containing DQM variables of different sizes.

1. No auxilliary variables

In this case all we need to do is to count the linear and quadratic degrees of freedom from the binary vari-

ables comprising each discrete variable, and find the size at which there are just enough degrees of freedom to implement all m^2 interaction terms. We first make an observation, terms which are either linear, or quadratic but between two binary variables which are used to encode the same discrete variable can only contribute a maximum of m degrees of freedom per variable. The reason for this is that the energy shifts these give are not sensitive to what any other variable is doing, and therefore can only contribute one degree of freedom per available value. In cases where there are sufficiently many of these degrees of freedom, we then need to show that there are at least $m^2 - 2m$ quadratic degrees of freedom which contain one binary variable used to encode each.

To understand mathematically why there is a limitation on the number of degrees of freedom which can be contributed by interactions within a single variable encoding, let us consider the general case of two variables of size m . In this case the QUBO terms can be written (using two index qubo variables where the first index i or j corresponds to a discrete variable encoding and the second index α or β corresponds to the qubit number within the discrete variable encoding) as

$$H_{\text{QUBO}} = \sum_{i,j}^{n_{\text{var}}} \sum_{\alpha,\beta} B_{(i,j,\alpha,\beta)} b_{i,\alpha} b_{j,\beta} \\ = \sum_{i,j}^{n_{\text{var}}} \sum_{\alpha} B_{(i,j,\alpha,\alpha)} b_{i,\alpha} b_{j,\alpha} + \sum_{i,j}^{n_{\text{var}}} \sum_{\alpha < \beta} (B_{(i,j,\alpha,\beta)} + B_{(i,j,\beta,\alpha)}) b_{i,\alpha} b_{j,\beta} \quad (12)$$

where $B_{(i,j,\alpha,\beta)}$ is a tensor used to store the QUBO terms used in the encoding in a similar way in which $D_{(i,j,\alpha,\beta)}$ is used to store the interactions between discrete variables and n_{var} is the number of binary variables

used to encode each discrete variable. We now make an observation, if we translate between the QUBO interactions and the energies of the encoded variables, we have

$$\sum_{i,j} B_{(i,j,\alpha,\alpha)} b_{i,\alpha} b_{j,\alpha} \leftrightarrow \sum_{k,l}^m D_{(k,l,\alpha,\alpha)} x_{k,\alpha} x_{l,\alpha} = \sum_k^m D_{(k,k,\alpha,\alpha)} x_{k,\alpha} \quad (13)$$

the second equality can be derived from the fact that each variable can only take one value, so therefore $x_{k,\alpha} x_{l,\alpha} = 0$ for all cases where $k \neq l$, along with the fact that $(x_{k,\alpha})^2 = x_{k,\alpha}$. The result is that, no matter how many $B_{(i,j,\alpha,\alpha)}$ degrees of freedom are available, they

can only contribute a maximum of m independent degrees of freedom for each discrete variable, since there are only m possible values of $x_{k,\alpha}$. Equation 14 shows where the different degrees of freedom come from for an interaction between two variables, giving a total of

$2 \min(m, \frac{n_{\text{var}}(n_{\text{var}}+1)}{2}) + n_{\text{var}}^2$ degrees of freedom for an interaction between two discrete variables of size m indexed

$$H_{\text{QUBO}} = \underbrace{\sum_{\gamma \in \alpha, \beta} \sum_{i,j}^{n_{\text{var}}} B_{(i,j,\gamma,\gamma)} b_{i,\gamma} b_{j,\gamma}}_{2 \min(m, \frac{n_{\text{var}}(n_{\text{var}}+1)}{2})} + \underbrace{\sum_{i,j}^{n_{\text{var}}} \sum_{\alpha < \beta} (B_{(i,j,\alpha,\beta)} + B_{(i,j,\beta,\alpha)}) b_{i,\alpha} b_{j,\beta}}_{n_{\text{var}}^2}. \quad (14)$$

We start with the domain-wall encoding, which uses $n_{\text{var}} = m - 1$ binary variable to encode a discrete variable of size m . Firstly, for $m > 2$, we find that indeed $\frac{(m-1)(m-2)}{2} > m$, so there are sufficient terms to gain m degrees of freedom per variable. Next we observe that $(m-1)^2 = m^2 - 2m + 1 > m^2 - 2m$, so again sufficient degrees of freedom, but with only one spare.

Next, we ask what happens when we remove one binary variable from even just one of the discrete variable encodings, we now have $(m-1)(m-2) = m^2 - 3m + 2$ degrees of freedom, for $m > 2$ we find that there are insufficiently many degrees of freedom (and will be even fewer if the number of binary variables are reduced further). We therefore conclude that unless auxilliary variables are added for each coupling, there is no way to construct a more efficient general interaction than the domain wall encoding. Note that this result is somewhat more substantial than the one in [16], which showed that the degrees of freedom which were used in the encoding were just sufficient, here we have shown that the domain-wall encoding is maximally efficient even if all linear and quadratic interactions are used.

B. Including auxilliary variables

We now ask whether more efficient encodings are possible if we allow each interaction to be supplemented by additional auxilliary variables which could, for example, be used to engineer higher-than-quadratic interactions, as shown in [13–15]. Since there are many different potential strategies for using auxilliary variables, and we do not want to consider every possibility independently, we instead base our argument on counting degrees of freedom, if there are insufficient degrees of freedom to independently control the energy of every configuration of a pair of variables, than no strategy can be used to construct general interactions[52]. We first use the results of the previous section to count the degrees of freedom before any auxilliary variables are added, if each discrete variable of size m uses $\lceil \log_2(m) \rceil \leq n_{\text{var}} < m - 1$ binary variables than there will be

$$D = m^2 - n_{\text{var}}^2 - 2 \min(m, \frac{n_{\text{var}}(n_{\text{var}}+1)}{2}) \quad (15)$$

with α and β each encoded into n_{var} binary variables.

degrees of freedom which will need to be added via linear terms on auxilliary variables and interactions between auxilliary variables. We will now assume that for each interaction between a pair of discrete variables n_{aux} auxilliary variables are included, which interact both with the discrete variables and between themselves. The goal of adding these variables is that each of them can be constrained to represent additional derived properties of the binary variables used to encode discrete variables, such as “majority votes” or parity values of subsets. Since the interactions between the auxilliary variables and the discrete variables will be used to control the values the auxilliaries take, they should not be counted toward the total available degrees of freedom, but both linear terms on the auxilliaries, and quadratic terms between them should, meaning that n_{aux} auxilliary variables give us $\frac{n_{\text{aux}}(n_{\text{aux}}+1)}{2}$ additional degrees of freedom.

We can therefore calculate the minimum necessary number of auxilliary variables needed to make up for the missing degrees of freedom by setting

$$\frac{n_{\text{aux}}(n_{\text{aux}}+1)}{2} \geq D.$$

By completing the square, we find the minimum number of auxilliary variables required to generate enough degrees of freedom

$$n_{\text{aux}} = \left\lceil \sqrt{2} \sqrt{D + \frac{1}{8}} - \frac{1}{2} \right\rceil, \quad (16)$$

where the bracketing symbols indicate ceiling, since this value must be an integer. The average number of binary variables used per discrete variable than becomes

$$n_{\text{bin}} = n_{\text{var}} + \frac{d}{2} n_{\text{aux}}, \quad (17)$$

where d is the average degree of the graph on which the problem is being solved. The condition for an encoding to be more efficient than the domain-wall encoding is therefore $n_{\text{bin}} < m - 1$, rearranging, we can find a critical degree below which an auxilliary variable based encoding becomes more efficient than the domain-wall encoding, this yields

$$d_{\text{crit}} = 2 \frac{m - 1 - n_{\text{var}}}{n_{\text{aux}}}. \quad (18)$$

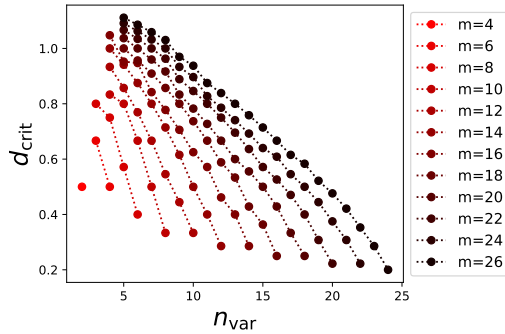


FIG. 3: Critical degree d_{crit} as defined in Eq. 19 for encodings using auxiliary variables with n_{var} binary variable per discrete variable for discrete variables sizes in the range $m = 4$ to $m = 26$. Only even values are plotted for easier visual interpretation, no significant even-odd effects have been observed. At all sizes shown here, choosing the minimum value of n_{var} (corresponding to a binary encoding) yields the highest d_{crit} and therefore the most efficient encoding, although not shown, a similar trend has been observed up to $m = 1000$.

Substituting in variables yields

$$d_{\text{crit}} = \sqrt{2} \frac{m - 1 - n_{\text{var}}}{\sqrt{m^2 - n_{\text{var}}^2 - 2 \min(m, \frac{n_{\text{var}}(n_{\text{var}}+1)}{2}) + \frac{1}{8}} - \frac{1}{2}}. \quad (19)$$

while applying this formula by hand to check every allowed value of n_{var} for a given value of m is impractical, especially for larger m , this value can be readily calculated by a computer. It is furthermore clear that in the limit of large m and small n_{var} , in other words for binary encodings with large m , the limiting value is $d_{\text{crit}} = \sqrt{2}$.

From applying eq. 19 for all values $3 < m \leq 1000$ we find firstly that the highest values of d_{crit} are always attained for binary encodings, in other words where the minimum number of binary variables are used to encode each discrete variable, this trend is shown for small m in fig. 3. As fig. 4 shows the maximum d_{crit} asymptotically approaches $\sqrt{2}$ from below.

Let us now consider what this critical value of degree means for real optimisation problems. Firstly, we are only interested in the connected components of the interaction graphs, since disconnected components can be solved separately. This limits the minimum average degree a graph can have based on the number of nodes (each of which correspond to DQM variables in this case), since the minimum connected graph with q nodes is either a star or line graph with $q - 1$ edges, and therefore an average degree of $d_q = 2\frac{q-1}{q}$. For example, a three node connected graph cannot have a degree less than $\frac{4}{3}$ and a four node connected graph cannot have degree less than $\frac{3}{2}$, since $\frac{3}{2} > \sqrt{2} > d_{\text{crit}}$, it follows that an auxiliary based encoding cannot be more efficient than the domain-wall encoding for problems on graphs with more than three nodes (and therefore containing more than three DQM variables). As discussed in [17] increasing the variable

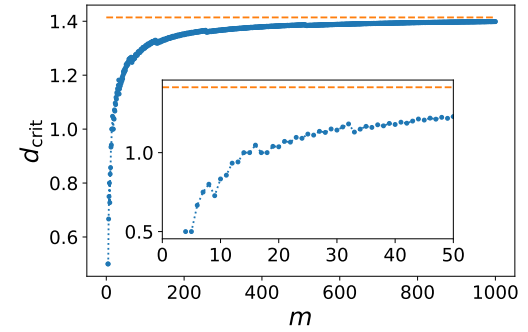


FIG. 4: Critical degree d_{crit} as defined in Eq. 19 for optimal encoding using auxiliary variables versus the size of the variable. Dashed line is a guide to the eye located at $d_{\text{crit}} = \sqrt{2}$. The inset is a zoom of the outer plot.

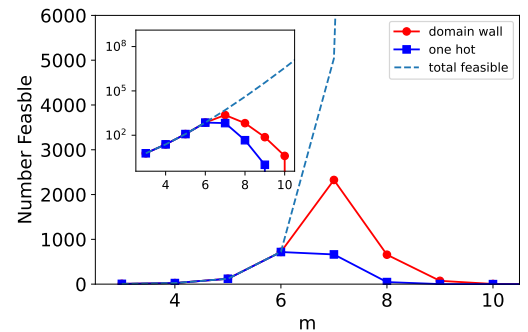


FIG. 5: Number of unique feasible solutions found for both encodings over all 10 embeddings versus m . Dashed line shows the total number of feasible solutions at each m value. The inset is the same plot but with a logarithmic scale on the y-axis.

size with a fixed number of variables is not a scalable way to perform quantum computation, so therefore the domain-wall encoding is the most efficient encoding for general interactions for all cases of practical interest.

While, strictly speaking, the interactions in the QAP are not completely arbitrary and have a set structure, we are not aware of any more efficient method to implement them beyond treating them as a specific case of a general encoding. It is worth remarking that the interactions between the variables are allowed to take arbitrary values in the travelling salesperson problem, so our results do imply that the domain-wall encoding is the most efficient way to encode the TSP with more than three cities.

C. Domain wall versus one-hot for quantum annealing

Now that we have established the domain-wall encoding as the optimal encoding for general DQM's we turn to the other main result of this paper, asking whether the annealing dynamics are favourable for a domain-wall en-

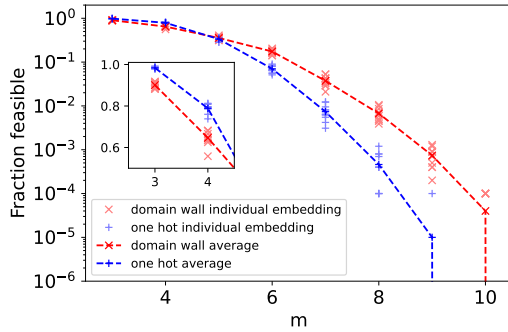


FIG. 6: Fraction of returned solutions which are feasible at different values of m . Full colour symbols indicate average over all 10 embeddings, while fainter symbols indicate values for individual embeddings. The inset shows a zoom on part of the plot with a linear y-axis to show the behavior before the crossover more clearly.

coded problem when compared to the same problem with a one-hot encoding. To do this, we first run the one-hot and domain-wall encoding of the unweighted QAP for 10 different embeddings with 10,000 anneals for each. As figure 5 shows, the domain-wall encoding is always able to find the same number or more feasible solutions in our experiments. However, as figure 6 shows, there is a crossover in terms of the probability that an individual annealing run yields a feasible solution, with one-hot performing better at smaller sizes and domain-wall performing better as the problem becomes larger. This is interesting because, while not in a particularly interesting regime (small sizes), this is the first case we are aware of where one hot is able to outperform domain wall by any metric. As we discuss later the cause of this crossover can be explained by a simple thermodynamic model.

In section III D in the spirit of the Kibble-Zurek Mechanism, we use these finite temperature models to estimate an effective temperature, and therefore determine which encoding yields dynamics which are more favourable to computation. We find that both thermodynamic and dynamical effects contribute to the superior performance of the domain-wall encoding. We also find that the chain strength chosen by a standard heuristic is actually lower for the one-hot encoding.

To understand the thermodynamics of the problems better, we first examine how temperature effects the QAP when using the domain-wall or one-hot encodings. To do this we perform a simple Metropolis algorithm on the two encodings at various temperatures for $m = 8$. While it won't necessarily be true for every problem, these converge well for the unweighted QAP. (Convergence of the Monte Carlo sampling is discussed in the appendix.) As Fig. 7 shows, at lower temperature the one-hot encoding performs better, but the domain-wall encoding performs better above a unitless temperature of $T \approx 0.5$. It is expected that at high temperatures, the domain-wall encoding should perform better, since the encoding uses m

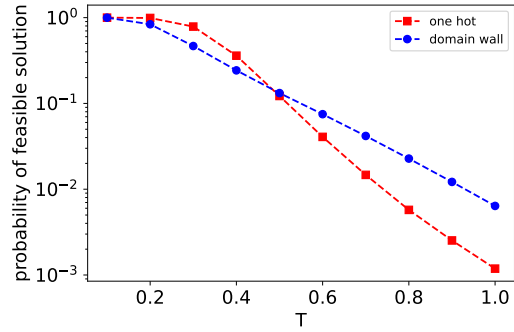


FIG. 7: Comparison of thermal probabilities for feasible solutions at different temperatures for domain-wall and one-hot encodings of $m = 8$ unweighted quadratic assignment problem. Temperature on this plot is in dimensionless units. All points represent Monte Carlo sampling with 10^7 samples, standard error and 95% error bars are both much smaller than the depicted symbols.

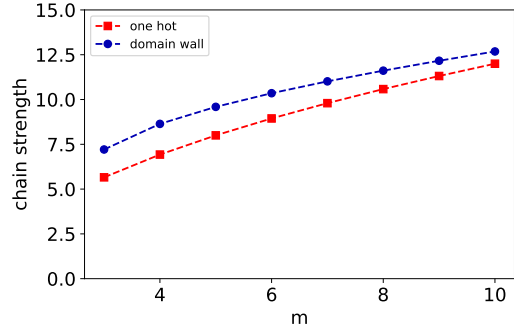


FIG. 8: Embedding chain strength calculated using the default uniform torque compensation heuristic for domain-wall and one-hot encodings.

fewer qubits, and therefore the solution space is 2^m times smaller, 256 times in the $m = 8$ case examined here

However, even assuming that the device always samples an equilibrium distribution at the same temperate, there are other considerations for device performance. To start with, the problem must be minor embedded in both cases, and the embedding chain strength required may not be the same for both encodings. Although experimentally we have seen that chain breaks are rare (this is also predicted by the large relative energy scale for the chains seen in figure 14), dynamic range limitations mean that the stronger the embedding chains needed, the lower the effective temperature of the encoded problem. For this study we have used the "uniform torque compensation" heuristic available in the Ocean software suite with default parameters [28]. Note that this heuristic does not depend on the embedding itself, only the pre-embedding problem. This heuristic estimates the necessary chain strength based on summing the couplings each logical variable experiences in quadrature. As fig. 8 shows, the heuristic consistently assigns stronger chain strengths for

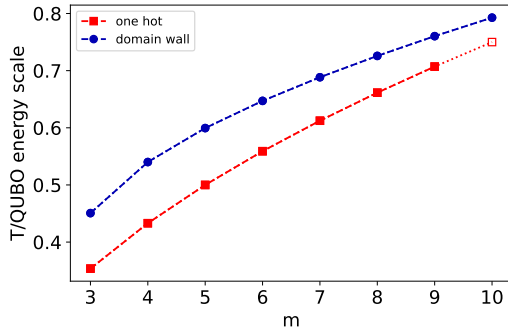


FIG. 9: Estimated effective temperature for one-hot and domain-wall encodings at different values of m . These values are calculated using a rough estimate of the unitless temperature and rescaling by the minor embedding chain strength. Since the heuristic has chosen a higher chain strength for the domain-wall encoding, this results in a higher effective temperature (unitless temperature of 0.063).

the domain-wall encoding, although the difference decreases as m increases. While beyond the scope of this investigation, it may be fruitful to examine whether different heuristics are more appropriate when domain-wall encoding is used, since the current heuristic was likely tested and tuned based on problem structures which are currently used, likely including one-hot constraints.

The final ingredient to investigate equilibrium effects on the annealing computer is an estimate of the temperature. While the physical temperature of these devices is well known at around 15 mK , the energy scale of the couplers at the point where the dynamics freeze is harder to estimate. For the purposes of this subsection we assume an energy of $\approx 5\text{ GHz}$. While this value is very approximate, and in practice the energy scale will change with the freeze time, choosing an approximate value of the correct order of magnitude for the device will allow investigation of relevant qualitative effects. Using this energy and physical temperature to calculate the the overall unitless temperature, we find $T = 0.063$. In section III D we use our modeling techniques to estimate the effective unitless temperature of the different encodings. However, at this stage an approximate value is sufficient to demonstrate the effects we want to show. Since some of the dynamic range is taken up by the embedding chains [25] the effective temperature we should use to model the solver needs to be further rescaled to take this into account, by about a factor of 10 in the $m = 8$ case. Fig. 9 shows the effective unitless temperature after rescaling effects from minor embedding are taken into account by rescaling the unitless temperature by the chain strength.

Using the same Metropolis techniques as before, we can estimate the probability of feasible solutions at different values of m . The results are shown in Fig. 10. Again, we see a crossover: For smaller m the one-hot encoding performs better, but above $m = 7$ the domain-wall method performs better. This is consistent with previous results,

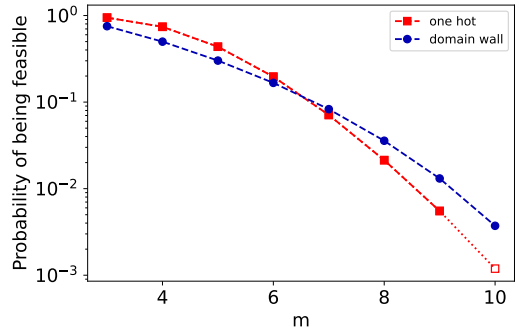


FIG. 10: Probability to find feasible solution based on thermal equilibrium model at different values of m . This plot includes effects of minor embedding and assumes freezing at a fixed value of $B = 5\text{ GHz}$ and a temperature of $15\text{ mK} \approx 0.31\text{ GHz}$. This plot is to illustrate the behaviour of the model, extracted values of the freeze time energy scales can be found in figure 14. All data points are based on 10^7 samples, 95% confidence statistical errorbars are smaller than depicted symbols.

for smaller m the effective temperature is smaller, and the difference in effective temperatures is greater. For larger m , on the other hand, the larger solution space is likely to have an increased effect given both the fact that the effective temperature is higher, and the ratio of the sizes of the solution spaces doubles each time m is increased.

D. Effective temperature

In the previous section we examined the effect of encoding on success probability at thermal equilibrium. This thermal modelling can moreover be useful in evaluating the dynamics. In particular we can consider a model based on the Kibble-Zurek mechanism (KZM) [19–23, 34] where a system is approximated to remain in equilibrium until it approaches a phase transition and the dynamics suddenly freeze out. Furthermore, since it is the quantum fluctuations which mediate the dynamics, it is reasonable to assume that these have relatively little effect at the freezing point, and to a first approximation we consider the distribution at the freezing point to be a classical thermal distribution. This assumption may not be justified for all systems, particularly those which use “free variable” gadgets [21, 24, 35–38], where the transverse fields act at degenerate order in perturbation theory. It was further seen in [21], that for problems which do not have “free” variables (all variables having having type 0 or I spin-sign transitions in the language of that work), the effects of transverse field and thermal fluctuations were very similar.

Furthermore, all problems studied here are minor embedded, so therefore in many cases, multiple physical qubits must be flipped to change the value of a single

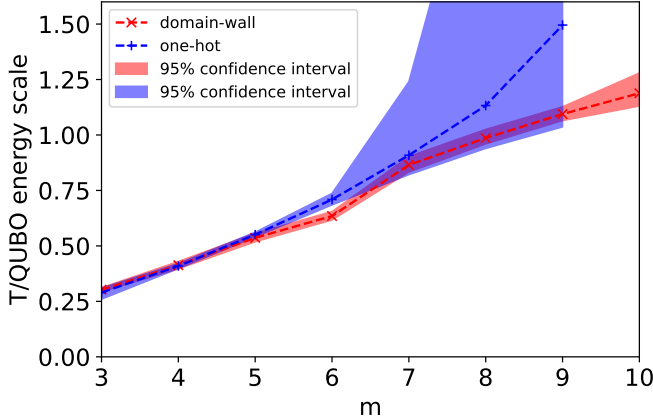


FIG. 11: Effective temperature compared to QUBO energy scale at different values of m for both encodings of the unweighted QAP. Methods for extracting the temperature are discussed in section IV. Note that the extremely large confidence intervals for one-hot at larger m are primarily due to few feasible solutions being found, at the extreme of only a single feasible solution in all 10^5 samples for $m = 9$.

logical variable, and the system must pass through high-energy ‘‘broken chain’’ states to do so. In other words, in a perturbative treatment similar to that used in [39], the minimum perturbative order at which the transverse field can have an effect is equal to the minimum number of qubits in an embedding chain. For one-hot encoding, all variables map to at least two qubits for $m > 6$, while for domain-wall these variables map to at least two qubits for $m > 7$.

For lower values of m , we need to compare the strength of the quantum and thermal fluctuations at the freeze time, which can be estimated by comparing the experimental probability of feasible solutions to our model. If thermal fluctuations are much stronger than quantum fluctuations then we are justified in our analysis. On the other hand, if it is the case that quantum fluctuations are on the order of thermal fluctuations, then a model which explicitly includes quantum fluctuations is necessary. Fortunately, as we show later in figure 14, our classical treatment is justified.

To estimate the temperature we take the measured probability of a feasible solution and perform bisection until the model and the experiment match well. We first extract the unitless ratio of the temperature over the energy scale of the optimisation problem, ignoring for the moment the dynamic range squeezing caused by the strong ferromagnetic chains needed for minor embedding. The result is shown in Fig. 11. From this figure we see little difference between the two encodings.

However, this figure does not tell the whole story, recall from Figs. 8 and 9 that the heuristic we have used to choose the chain strength has specified a significantly weaker chain strength for one-hot. To really understand the freezing time we must compare the temperature not

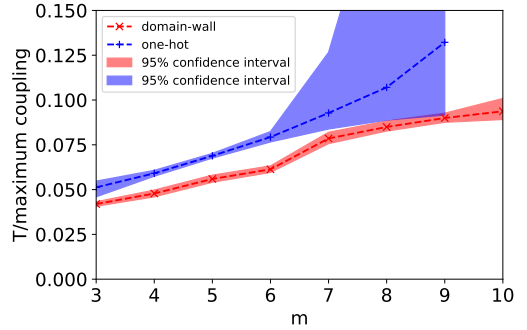


FIG. 12: Effective temperature compared to maximum possible coupling at different values of m for both encodings of the unweighted QAP. Methods for extracting the temperature are discussed in section IV.

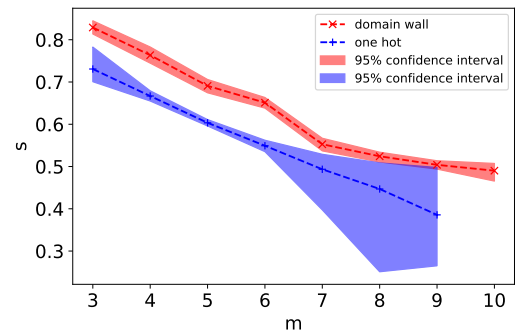


FIG. 13: Extracted value of annealing parameter s at the freezing point for one-hot and domain-wall encodings of the unweighted QAP at different sizes. Methods for extracting the value of s are discussed in section IV.

to the QUBO energy strength, but to the maximum coupling used for the problem. As Fig. 12 shows, once the overall energy scale is taken into account, it is clear that the domain-wall encoding is in fact sampling at a lower effective temperature. This result suggests that, the domain-wall encoding does indeed lead to later freezing of the dynamics (as depicted in figure 13) and therefore a lower effective temperature.

A later freezing time shows something fundamental about our encoding, namely that the fundamental dynamics of the annealing are facilitated by this encoding. The dynamics are more resistant to localization than they would be in one-hot. Since problem encoding is traditionally considered the domain of computer scientists, there is little (in fact no previous work we are aware of) research on how the physics is affected by how problems are encoded, this result shows that this is in fact an important consideration, and considering the encoding and device physics as completely separate ‘‘layers’’ of the device operation may not be an optimal approach.

We now return to the question of whether we were justified in ignoring quantum fluctuations in our final model of the distribution. To do this, we need to show two

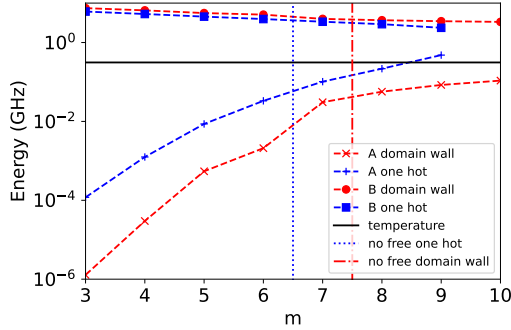


FIG. 14: $A(s)$ and $B(s)$ energy scales at freeze time for the one-hot and domain-wall encoded unweighted QAP for different values of m . This is compared to the approximate temperature of $15\text{ mK} \approx 0.31\text{ GHz}$. Vertical lines (labeled “no free one hot” and “no free domain wall”) indicated the transition between values of m where at least one variable in at least one embedding maps to a single qubit, and where every one maps to at least two qubits.

things, firstly we need to show that for regimes where some variables map only to single qubits the transverse field energy scale $A(s)$ is much lower than the temperature of the device, so that thermal fluctuations will have a stronger effect than quantum fluctuations. Secondly, in the regime where all variables are mapped to at least two qubits, we still need to show that $A(s) \ll B(s)$ so that treating the effect of the transverse field at second order in perturbation theory is justified. Again we can calculate these values by matching the success probability to an effective temperature in the thermal model and then extrapolating the energy scales based on an approximate temperature of 15 mK . As Figure 14 shows, these criteria are met for all problems studied here, suggesting that this model should at least be a reasonable approximation (although this approximation is more questionable for one-hot at large m values).

IV. EXPERIMENTAL AND NUMERICAL METHODS

All experiments reported here were performed on a D-Wave Advantage 1.1 quantum annealing computer which was accessed through Amazon Web Services between the dates of June 22 and June 25 2021. All experiments were performed using the default device settings, including an annealing time of $20\text{ }\mu\text{s}$. Spin reversal transforms (also known as gauge averaging) were not used. For each value of m , ten separate embeddings were used with 10,000 anneals for each (for a total of 100,000 anneals at each size). In addition to the sizes reported here, sizes $m = 11$ and $m = 12$ were also tested, but no feasible solutions were found with either encoding in all 100,000 anneals. Furthermore, no experimental results are reported for one-hot with $m = 10$ because no feasible solutions were found

experimentally (for this reason we have left the $m = 10$ symbol for one-hot unfilled on relevant theory plots). The annealing schedule and other device parameters were obtained from the D-Wave user forums [40].

Effective temperatures for figures 11 and 12 were calculated by bisection using Monte Carlo. An initial temperature range was defined to run between $T_{\min} = 0$ and $T_{\max} = 2.5$ times the QUBO energy scale, then with 10^7 samples at the midpoint of the range to test if the fraction of feasible solutions exceeded what was observed experimentally, if it did than a new T_{\min} was defined to be this midpoint if not T_{\max} was assigned the midpoint value. This routine was performed for 15 iterations for each point. The 95% confidence bounds were calculated using the same procedure, but using an experimental success probability which was the measured value plus or minus twice the experimental standard error. Quantities A , B and s were then calculated by first extracting B based on a physical temperature of approximately $15\text{ mK} \approx 0.31\text{ GHz}$, A and s were calculated by performing linear interpolation against an annealing schedule provided on the D-Wave user forums [40]. Note that these schedules are approximate and according to the source may deviate by up to 30%. Monte Carlo sampling was performed using standard Metropolis updates starting from a feasible solution. The number of Monte Carlo samples is based on the number of **attempted** updates (we have used 10^7 to ensure statistical convergence and to ensure sufficiently many updates for the algorithm to achieve equilibrium, see appendix), so cases where the update was attempted but not performed would still count as separate samples.

V. DISCUSSIONS AND CONCLUSIONS

We have shown two important results related to the domain-wall encoding, and answered two key open questions. Firstly we have shown that for DQMs with general interactions, no better (quadratic) encoding can exist for problems with more than 3 variables, which comprise all interesting optimisation problems for quantum computing applications. This result applies to any algorithm where a unary encoding of single variables is desired, this includes quantum annealing, but not exclusively, for example this method could equally well save qubits in gate model optimisation and quantum inspired algorithms. Secondly, we have experimentally verified theoretical predictions that domain-wall encoding will lead to more favourable dynamics in physical implementations of quantum annealing. The first of these results is important because it implies that there is no need to search for more efficient general DQM encodings, and any future efforts can be focused on encoding specific structures of interactions. The second of these results highlights the importance of considering the physical dynamics the system will undergo when designing problem encodings.

While problem encoding has traditionally been considered

ered to be a computer science topic, our results suggest that there is important interplay between the encoding and the underlying physics, therefore the physics of the device needs to be considered when designing problem encodings.

The goal of this study was not to fully understand how to optimise the performance of the device, so it is worth noting that other factors, such as anneal time will also change these properties. In particular, our results suggest that especially for larger QAP problems, annealing for longer to gain a later freeze time and therefore a lower effective temperature is likely to be fruitful. It is important to note that, while this work does provide useful relative comparisons of encodings, as with the work in [10], it does not test the ultimate performance limits of the devices [53], so that the experiments remain simple. In particular the features which allow the minor embedding chains to effectively be twice as strong would probably improve the results substantially [41], also tuning of parameters like the anneal time may have led to further improvement (this feature requires substantial calibration time so was not used in our experiment since we care about relative rather than absolute performance).

While the experimental portion of this work was performed on a quantum annealing computer due to the larger sizes of devices available, other settings of particular interest are gate model settings, it is comparatively easier to engineer higher than quadratic interactions within this setting (typically at the cost of more circuit depth) leading to complicated tradeoffs [18], but it is likely that in at least some cases unary encoding of single variables are desired. There are also two-body drivers which drive directly between valid states for both one hot [42] and domain wall [16], but typically two qubit gates are noisier so this is again a tradeoff. In cases where unary encodings are used our work has a potentially strong impact, optimal QAOA [43] will mimic quantum annealing [44] and therefore be subject to similar “freeze time” dynamics to those discussed here. The concept of a “freeze time” in fact affects any a system approaches a phase transition [19, 20] so may be relevant to other cases as well, for example in VQE [45] where the desired state lies near a phase transition. Furthermore, coherent Ising machines [46, 47] and digital annealers [48, 49] both are limited to quadratic interactions and will be approximated by similar “freeze time” models to the ones we use here.

VI. ACKNOWLEDGMENTS

All authors were entirely supported in writing this paper by Quantum Computing Inc. which also provided the necessary machine time.

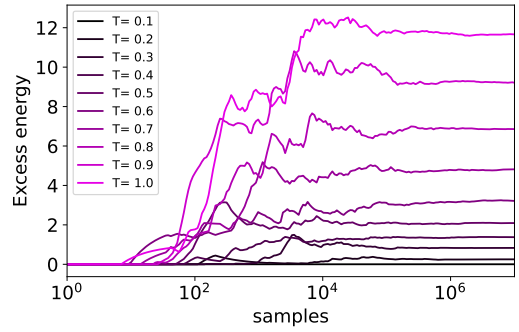


FIG. 15: Running average of excess energy (compared to a feasible state) for an unweighted $m = 10$ QAP with up to 10^7 samples at different dimensionless temperatures encoded using the domain-wall encoding. Note logarithmic scale of x-axis.

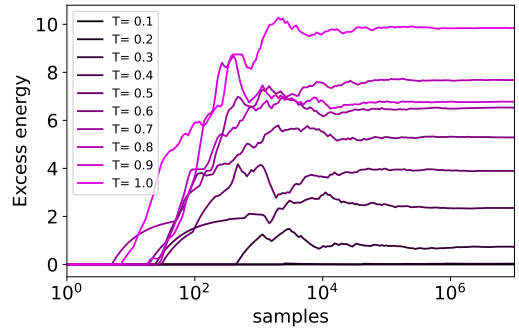


FIG. 16: Running average of excess energy (compared to a feasible state) for an unweighted $m = 10$ QAP with up to 10^7 samples at different dimensionless temperatures, encoding using one-hot encoding. Note logarithmic scale of x-axis.

Appendix: Convergence of Monte Carlo sampling

The experimental data analysis in this work relies on the numerical Monte Carlo sampling being able to accurately sample a thermal distribution. While the high level of symmetry of the unweighted QAP suggests that equilibration should be relatively quick, we should still verify this numerically. As we can see from figures 15 and 16, even for the largest system here, complete convergence has occurred after 10^6 samples at all temperatures, and a fair quality approximate convergence has occurred even by 10^5 samples.

While these plots show convergence, the remaining question is rather subsequent runs will typically reach a similar equilibrium. To check this we perform for each temperature and both encodings ten times with 10^7 samples each. We then find the ratio of the standard deviation divided by the mean over each set of ten samples. Standard deviation is used rather than standard error, since many of our methods rely on a single set of 10^7 samples. What we find is that for most cases

T	domain wall	one-hot
0.1	0.17	N/A
0.2	0.016	0.039
0.3	0.0063	0.013
0.4	0.0030	0.004
0.5	0.0069	0.0028
0.6	0.095	0.0012
0.7	0.0032	0.095
0.8	0.046	0.080
0.9	0.00316	0.0013
1.0	0.11	0.062

TABLE I: Standard deviation (NB **not** standard error) over mean energy value for 10 Monte Carlo runs with 10^7 samples each at different temperatures for both encodings.

the standard error relative to mean is small with a few notable exceptions. The sampling is not reliable below $\frac{T}{\text{QUBO energy}} = 0.2$ for either encoding, the domain-wall

encoding shows a large normalized standard deviation at $\frac{T}{\text{QUBO energy}} = 0.1$, while the ratio is not defined for the one-hot encoding because in some cases no unfeasible solutions were found. Fortunately this is not very relevant to our experimental analysis since the lowest experimentally fitted value of unitless temperature is around $\frac{T}{\text{QUBO energy}} \approx 0.25$ (see figure 11). It is likely that this relatively large normalized standard deviation is due to the fact the the mean energy is very small. The normalized standard deviation for $\frac{T}{\text{QUBO energy}} = 1.0$ for domain wall is also relatively large, and might somewhat affect the accuracy of the extracted temperature for $m = 10$, but this point cannot change our key conclusions because there is no one-hot data to compare with. We have not checked temperatures above $\frac{T}{\text{QUBO energy}} = 1.0$ but the only experimental value which significantly exceeds this temperature is the one-hot sample at $m = 9$, since this point already has a large experimental standard error, it is not relevant to check that the contribution to the error from sampling is significant.

[1] A. Crispin and A. Syrichas. Quantum annealing algorithm for vehicle scheduling. In *2013 IEEE International Conference on Systems, Man, and Cybernetics*, pages 3523–3528, Oct 2013.

[2] Florian Neukart, Gabriele Compostella, Christian Seidel, David von Dollen, Sheir Yarkoni, and Bob Parney. Traffic flow optimization using a quantum annealer. *Frontiers in ICT*, 4:29, 2017.

[3] Sheir Yarkoni, Florian Neukart, Eliane Moreno Gomez Tagle, Nicole Magiera, Bharat Mehta, Kunal Hire, Swapnil Narkhede, and Martin Hofmann. *Quantum Shuttle: Traffic Navigation with Quantum Computing*, page 22–30. Association for Computing Machinery, New York, NY, USA, 2020.

[4] Daniel O’Malley. An approach to quantum-computational hydrologic inverse analysis. *Scientific Reports*, 8(1):6919, 2018.

[5] Alejandro Perdomo-Ortiz, Neil Dickson, Marshall Drew-Brook, Geordie Rose, and Alan Aspuru-Guzik. Finding low-energy conformations of lattice protein models by quantum annealing. *Scientific Reports*, 2(571), 2012.

[6] Vikram Khipple Mulligan, Hans Melo, Haley Irene Merritt, Stewart Slocum, Brian D. Weitzner, Andrew M. Watkins, P. Douglas Renfrew, Craig Pelissier, Paramjit S. Arora, and Richard Bonneau. Designing peptides on a quantum computer. *bioRxiv*, 2020.

[7] Christian F. A. Negre, Hayato Ushijima-Mwesigwa, and Susan M. Mniszewski. Detecting multiple communities using quantum annealing on the d-wave system. *PLOS ONE*, 15(2):1–14, 02 2020.

[8] Hayato Ushijima-Mwesigwa, Christian F. A. Negre, and Susan M. Mniszewski. Graph partitioning using quantum annealing on the d-wave system, 2017. arXiv:1705.03082.

[9] Zsolt Tabi, Kareem H. El-Safty, Zsófia Kallus, Péter Hágá, Tamás Kozsik, Adam Glos, and Zoltán Zimborás. Quantum optimization for the graph coloring problem with space-efficient embedding. 2020.

[10] Jie Chen, Tobias Stollenwerk, and Nicholas Chancellor. Performance of domain-wall encoding for quantum annealing. *IEEE Transactions on Quantum Engineering*, 2:1–14, 2021.

[11] Yongcheng Ding, Xi Chen, Lucas Lamata, Enrique Solano, and Mikel Sanz. Implementation of a hybrid classical-quantum annealing algorithm for logistic network design. *SN Computer Science*, 2(2):68, Feb 2021.

[12] John Preskill. Quantum Computing in the NISQ era and beyond. *Quantum*, 2:79, August 2018.

[13] N. Chancellor, S. Zohren, P. A. Warburton, S. C. Benjamin, and S. Roberts. A direct mapping of max k-sat and high order parity checks to a chimera graph. *Scientific Reports*, 6(1):37107, Nov 2016.

[14] Martin Leib, Peter Zoller, and Wolfgang Lechner. A transmon quantum annealer: decomposing many-body Ising constraints into pair interactions. *Quantum Science and Technology*, 1(1):015008, 2016.

[15] Nikesh S. Dattani. Quadratization in discrete optimization and quantum mechanics, 2019. arXiv:1901.04405.

[16] Nicholas Chancellor. Domain wall encoding of discrete variables for quantum annealing and QAOA. *Quantum Science and Technology*, 4(4):045004, aug 2019.

[17] Robin Blume-Kohout, Carlton M. Caves, and Ivan H. Deutsch. Climbing mount scalable: Physical resource requirements for a scalable quantum computer. *Foundations of Physics*, 32(11):1641–1670, Nov 2002.

[18] Nicolas P. D. Sawaya, Tim Menke, Thi Ha Kyaw, Sonika Johri, Alán Aspuru-Guzik, and Gian Giacomo Guerreschi. Resource-efficient digital quantum simulation of d-level systems for photonic, vibrational, and spin-s hamiltonians. *npj Quantum Information*, 6(1):49, Jun 2020.

[19] T W B Kibble. Topology of cosmic domains and strings. *Journal of Physics A: Mathematical and General*,

9(8):1387–1398, aug 1976.

[20] W.H. Zurek. Cosmological experiments in condensed matter systems. *Physics Reports*, 276(4):177–221, 1996.

[21] Nicholas Chancellor, Gabriel Aeppli, and Paul A. Warburton. Experimental freezing of mid-evolution fluctuations with a programmable annealer, 2016. arXiv:1605.07549.

[22] Yuki Bando, Yuki Susa, Hiroki Oshiyama, Naokazu Shiba, Masayuki Ohzeki, Fernando Javier Gómez-Ruiz, Daniel A. Lidar, Sei Suzuki, Adolfo del Campo, and Hidetoshi Nishimori. Probing the universality of topological defect formation in a quantum annealer: Kibble-zurek mechanism and beyond. *Phys. Rev. Research*, 2:033369, Sep 2020.

[23] Phillip Weinberg, Marek Tylutki, Jami M. Rönkkö, Jan Westerholm, Jan A. Åström, Pekka Manninen, Päivi Törmä, and Anders W. Sandvik. Scaling and diabatic effects in quantum annealing with a d-wave device. *Phys. Rev. Lett.*, 124:090502, Mar 2020.

[24] N. G. Dickson et al. Thermally assisted quantum annealing of a 16-qubit problem. *Nature Communications*, 4(1):1903, 2013.

[25] Tameem Albash, Victor Martin-Mayor, and Itay Hen. Temperature scaling law for quantum annealing optimizers. *Phys. Rev. Lett.*, 119:110502, Sep 2017.

[26] Vicky Choi. Minor-embedding in adiabatic quantum computation: I. the parameter setting problem. *Quantum Information Processing*, (7):193–209, 2008.

[27] Vicky Choi. Minor-embedding in adiabatic quantum computation: II. minor-universal graph design. *Quantum Information Processing*, 10:343, 2011.

[28] Documentation on D-Wave Uniform Torque Compensation tool, Accessed 2021-19-01. url: https://docs.ocean.dwavesys.com/projects/system/en/stable/reference/generated/dwave.embedding.chain_strength.uniform_torque_compensation.html.

[29] Hedayat Alghassi, Raouf Dridi, and Sridhar Tayur. Graver bases via quantum annealing with application to non-linear integer programs, 2019. arXiv:1902.04215.

[30] Steven Abel, Nicholas Chancellor, and Michael Spannowsky. Quantum computing for quantum tunnelling. arXiv:2003.07374, 2020.

[31] Steven Abel and Michael Spannowsky. Observing the fate of the false vacuum with a quantum laboratory, 2020. arXiv:2006.06003.

[32] Raouf Dridi, Hedayat Alghassi, and Sridhar Tayur. A novel algebraic geometry compiling framework for adiabatic quantum computations, 2018. arXiv:1810.01440.

[33] David Joseph, Adam Callison, Cong Ling, and Florian Mintert. Two quantum ising algorithms for the shortest-vector problem. *Phys. Rev. A*, 103:032433, Mar 2021.

[34] Bogdan Damski. The simplest quantum model supporting the kibble-zurek mechanism of topological defect production: Landau-zener transitions from a new perspective. *Phys. Rev. Lett.*, 95:035701, Jul 2005.

[35] Sergio Boixo, Tameem Albash, Federico M. Spedalieri, Nicholas Chancellor, and Daniel A. Lidar. Experimental signature of programmable quantum annealing. *Nature Communications*, 4(1):2067, Jun 2013.

[36] Tameem Albash, Walter Vinci, Anurag Mishra, Paul A. Warburton, and Daniel A. Lidar. Consistency tests of classical and quantum models for a quantum annealer. *Phys. Rev. A*, 91:042314, Apr 2015.

[37] Nicholas Chancellor and Viv Kendon. Experimental test of search range in quantum annealing. *Phys. Rev. A*, 104:012604, Jul 2021.

[38] Nicholas Chancellor. Fluctuation-guided search in quantum annealing. *Phys. Rev. A*, 102:062606, Dec 2020.

[39] A. Ben Dodds, Viv Kendon, Charles S. Adams, and Nicholas Chancellor. Practical designs for permutation-symmetric problem hamiltonians on hypercubes. *Phys. Rev. A*, 100:032320, Sep 2019.

[40] D-Wave Systems Inc. QPU specific anneal schedules, Accessed 26 July 2021. url: <https://support.dwavesys.com/hc/en-us/articles/360005267253-QPU-Specific-Anneal-Schedules>.

[41] Source code for `dwave.system.composites.virtual_graph`, Accessed 2021-19-01. https://docs.ocean.dwavesys.com/en/stable/_modules/dwave/system/composites/virtual_graph.html.

[42] Stuart Hadfield, Zhihui Wang, Bryan O’Gorman, Eleanor G. Rieffel, Davide Venturelli, and Rupak Biswas. From the quantum approximate optimization algorithm to a quantum alternating operator ansatz. *Algorithms*, 12(2), 2019.

[43] Edward Farhi, Jeffrey Goldstone, and Sam Gutmann. A quantum approximate optimization algorithm, 2014. arXiv:1411.4028.

[44] Lucas T. Brady, Christopher L. Baldwin, Aniruddha Bapat, Yaroslav Kharkov, and Alexey V. Gorshkov. Optimal protocols in quantum annealing and quantum approximate optimization algorithm problems. *Phys. Rev. Lett.*, 126:070505, Feb 2021.

[45] Alberto Peruzzo, Jarrod McClean, Peter Shadbolt, Man-Hong Yung, Xiao-Qi Zhou, Peter J. Love, Alán Aspuru-Guzik, and Jeremy L. O’Brien. A variational eigenvalue solver on a photonic quantum processor. *Nature Communications*, 5(1):4213, Jul 2014.

[46] Peter L. McMahon, Alireza Marandi, Yoshitaka Haribara, Ryan Hamerly, Carsten Langrock, Shuhei Tamate, Takahiro Inagaki, Hiroki Takesue, Shoko Utsunomiya, Kazuyuki Aihara, Robert L. Byer, M. M. Fejer, Hideo Mabuchi, and Yoshihisa Yamamoto. A fully-programmable 100-spin coherent ising machine with all-to-all connections. *Science*, 2016.

[47] Takahiro Inagaki, Yoshitaka Haribara, Koji Igarashi, Tomohiro Sonobe, Shuhei Tamate, Toshimori Honjo, Alireza Marandi, Peter L. McMahon, Takeshi Umeki, Koji Enbusu, Osamu Tadanaga, Hirokazu Takenouchi, Kazuyuki Aihara, Ken-ichi Kawarabayashi, Kyo Inoue, Shoko Utsunomiya, and Hiroki Takesue. A coherent ising machine for 2000-node optimization problems. *Science*, 354(6312):603–606, 2016.

[48] Masanao Yamaoka, Chihiro Yoshimura, Masato Hayashi, Takuwa Okuyama, Hidetaka Aoki, and Hiroyuki Mizuno. Ising computer. *Hitachi Review*, 65(6):156–160, 2016.

[49] Fujitsu Labs Ltd. Fujitsu laboratories and university of toronto enter strategic partnership, 2017.

[50] Wolfgang Lechner, Philipp Hauke, and Peter Zoller. A quantum annealing architecture with all-to-all connectivity from local interactions. *Science Advances*, 1(9), 2015.

[51] we use the term binary variable here because problem mapping processes, such as minor embedding, parity encoding (i.e. [50]), or error correction codes may mean that the value of a single binary variable is stored over multiple physical qubits

[52] We are not sure if the converse of this statement is true,

in other words, we aren't aware of a construction which always works when sufficient degrees of freedom are available. Calculations done in this way should therefore be viewed as bounds

[53] potential routes to improvement are discussed in section III D of [10]